

Hexagonal and Prismatic Nanowalled ZnO Microboxes

Fenghua Zhao,[†] Wenjiao Lin,[†] Mingmei Wu,^{*†} Ningsheng Xu,[†] Xianfeng Yang,[†] Z. Ryan Tian,^{**‡} and Qiang Su[†]

The State Key Laboratory of Optoelectronic Materials and Technologies, School of Chemistry and Chemical Engineering, School of Physics and Engineering, Sun Yat-Sen (Zhongshan) University, Guangzhou 510275, People's Republic of China, and Department of Chemistry and Biochemistry, University of Arkansas, Fayetteville, Arkansas 72701

Received October 24, 2005

We hereby report hydrothermal syntheses of new microstructures of semiconducting ZnO. Single-crystalline prismatic ZnO microboxes formed by nanowalls and hexagonal hollow microdisks closed by plates with micron-sized inorganic fullerene-like structures have been made in a base-free medium through a one-step hydrothermal synthesis with the help of *n*-butanol (NB). Structures and morphologies of the products were confirmed by results from powder X-ray diffraction and scanning electron microscopy. NB has been found to play a crucial role in the growth of these hollow structures. It is indicated that these hollow ZnO crystals were grown from redissolution of interiors. These ZnO microboxes exhibit a band emission in the visible range, implying the possession of a high content of defects.

Introduction

To fulfill the increasing demands of high efficiency in chemical reactions and optoelectronic transition, much effort has been devoted to the synthesis of new nanomaterials with unusual nanostructures.¹ Compared with the insulating silicate and aluminosilicate frameworks, these porous and tubular-structured nanomaterials have been found to be useful in separation, ion exchange, catalysis, guest chemistry, and electrical and optical technology.^{2–8}

Topologically, tubular structures could be formed by curled layered materials.^{5–7} Thus, a variety of new tubular structures

of oxides and sulfides have been made from solutions.^{6,7,9–11} Quite a few prismatic tubes that cannot be formed by curled lamellar structures have also been reported.^{7,12–24} These non-carbon tubular structures have either one or two open ends.^{7,12–24} To date, very few examples of prismatic and single-crystalline inorganic microboxes and hollow microdisks with fullerene-like structures have been published.^{25,26}

* To whom correspondence should be addressed. E-mail: ceswmm@sysu.edu.cn (M.M.W.), rtian@uark.edu (Z.R.T.). Tel: 86-20-84036766 (M.M.W.). Fax: 86-20-84036766 (M.M.W.).

[†] Sun Yat-Sen (Zhongshan) University.

[‡] University of Arkansas.

- (1) (a) Murphy, C. J.; Jana, N. R. *Adv. Mater.* **2002**, *14*, 80–82. (b) Vayssieres, L.; Hagfeldt, A.; Lindquist, S. E. *Pure Appl. Chem.* **2000**, *72*, 47–52. (c) Peng, X.-G.; Manna, L.; Yang, W.-D.; Wickham, J.; Scher, E.; Kadavanich, A.; Alivisatos, A. P. *Nature* **2000**, *404*, 59–61. (d) Bommel, K. J. C.; Friggeri, A.; Shinkai, S. *Angew. Chem., Int. Ed.* **2003**, *42*, 980–999. (e) Bauerlein, E. *Angew. Chem., Int. Ed.* **2003**, *42*, 614–641. (f) Murugavel, R.; Walawalkar, M. G.; Dan, M.; Roesky, H. W.; Rao, C. N. R. *Acc. Chem. Res.* **2004**, *37*, 763–774. (g) Fernandez-Garcia, M.; Martinez-Arias, A.; Hanson, J. C.; Rodriguez, J. A. *Chem. Rev.* **2004**, *104*, 4063–4104. (h) Mendes, P. M.; Preece, J. A. *Curr. Opin. Colloid Interface Sci.* **2004**, *9*, 236–248.
- (2) (a) Tosheva, L.; Valtchev, V. P. *Chem. Mater.* **2005**, *17*, 2494–2513. (b) Scott, B. J.; Wirnsberger, G.; Stucky, G. D. *Chem. Mater.* **2001**, *13*, 3140–3150.
- (3) (a) Soler-illia, G. J. D.; Sanchez, C.; Lebeau, B.; Patarin, J. *Chem. Rev.* **2002**, *102*, 4093–4138. (b) Davis, M. E. *Nature* **2002**, *417*, 813–821.

- (4) (a) Yu, C. Z.; Tian, B. Z.; Zhao, D. Y. *Curr. Opin. Solid State Mater. Sci.* **2003**, *7*, 191–197. (b) Feng, P. Y.; Bu, X. H.; Zheng, N. F. *Acc. Chem. Res.* **2005**, *38*, 293–303. (c) Mohanan, J. L.; Arachchige, I. U.; Brock, S. L. *Science* **2005**, *307*, 397–400. (d) Gao, F.; Lu, Q. Y.; Zhao, D. Y. *Adv. Mater.* **2003**, *15*, 739–742. (e) Li, H. L.; Laine, A.; O'Keeffe, M.; Yaghi, O. M. *Science* **1999**, *283*, 1145–1147. (f) Zhang, Q. M.; Li, Y.; Huang, F. Z.; Gu, Z. N. *J. Mater. Sci. Lett.* **2001**, *20*, 1233–1235. (g) Yang, P. D.; Zhao, D. Y.; Margolese, D. I.; Chmelka, B. F.; Stucky, G. D. *Nature* **1998**, *396*, 152–155.
- (5) (a) Zhou, O.; Shimoda, H.; Gao, B.; Oh, S. J.; Fleming, L.; Yue, G. Z. *Acc. Chem. Res.* **2002**, *35*, 1045–1053. (b) Ouyang, M.; Huang, J.-L.; Lieber, C. M. *Acc. Chem. Res.* **2002**, *35*, 1018–1025. (c) Baughman, R. H.; Zakhidov, A. A.; de Heer, W. A. *Science* **2002**, *297*, 787–792.
- (6) (a) Rao, C. N. R. *Dalton Trans.* **2003**, *1*, 1. (b) Tenne, R. *Angew. Chem., Int. Ed.* **2003**, *42*, 5124–5132. (c) Patzke, G. R.; Krumeich, F.; Nesper, R. *Angew. Chem., Int. Ed.* **2002**, *41*, 2446–2461. (d) Tremel, W. *Angew. Chem., Int. Ed. Engl.* **1999**, *38*, 2175–2179. (e) Rao, C. N. R.; Tenne, R.; Terrones, E. M.; Terrones, H. In *Nanotechnology of Carbon and Related Materials, Philosophical Transactions: Mathematical, Physical and Engineering Sciences*; Royal Society: London, 2004. (f) Remskar, M. *Adv. Mater.* **2004**, *16*, 1497–1504.
- (7) Xia, Y. N.; Yang, P. D.; Sun, Y. G.; Wu, Y. Y.; Mayers, B.; Gates, B.; Yin, Y. D.; Kim, F.; Yan, Y. Q. *Adv. Mater.* **2003**, *15*, 353–389.
- (8) Steinhart, M.; Wehrspohn, R. B.; Gosele, U.; Wendorff, J. H. *Angew. Chem., Int. Ed.* **2004**, *43*, 1334–1344.

No successful synthesis of highly crystalline and hexagonally prismatic inorganic microboxes has been reported.

ZnO is a wide-band-gap group II–VI compound semiconductor ($E_g = 3.37$ eV). It can be used as catalytic, piezoelectric, dielectric, and optical materials in chemical sensing, solid-state lasing, and light emission.^{13–17,27–41} These ZnO crystals from either high-temperature vapor deposition

or low-temperature solution chemistry could take numerous morphologies including grains,^{30,31} rods (wires and columns),^{38–42} belts,^{43,44} rings,^{44,45} disks,⁴⁵ polyhedral microcages,⁴⁶ tubes,^{14–20,29,33} and complex structures.^{35,36,41,47,48} Yan and co-workers prepared cylindrical and closed-end ZnO nanotubes from ZnO nanoparticles through self-assembly using ethanol as the cosolvent with the help of NH_3 .³³ Inorganic and organic bases are commonly used in these solution syntheses. A base-free approach has been reported to prepare ZnO nanoparticles from precursory layered hydroxide of zinc acetate [$\text{LHZA}; \text{Zn}_5(\text{OH})_8(\text{CH}_3\text{COO})_2 \cdot 2\text{H}_2\text{O}$] under very mild conditions.^{30,31,49}

Hydrothermal treatment as a typical solution approach has been extensively studied for growing ZnO single crystals with a variety of morphologies,^{19,20,33–37,42,45,47} including hexagonal microtubes,^{19,20} hard nanodisks,⁴⁵ etc. These prismatic ZnO microtubes, hydrothermally grown on a substrate, have at least one open end.^{19,20} It was proposed that three-dimensional arrays of ZnO microtubes with open tops were produced from the redissolution of the metastable (001) faces of as-grown microrods.¹⁹ In this Article, hexagonally prismatic hollow microboxes and closed-end microdisks of ZnO have been synthesized via a facile one-step hydrothermal route. These microboxes exhibit a strong wide emission band in the visible range.

Experimental Section

1. Preparation. Solid zinc acetate (ZnAc_2) was dissolved in distilled water to prepare 1.0 mol L^{-1} of a transparent aqueous solution (ZA) as the zinc source. ZA was dropped into *n*-butanol (NB) under stirring to form a clear solution (CS). The stirring time was about 30 min. The concentration of ZnAc_2 in the feedstock was confirmed with the addition volumes of ZA (V_{ZA}) and NB (V_{NB}), respectively. The total volume of V_{ZA} and V_{NB} was fixed at 4.0 mL as the feedstock for the hydrothermal reaction. A Teflon liner (20 mL) was filled with such a volume of CS for the autoclave treatment at an elevated temperature for a certain period of time. The product was collected on an ultrasonically washed ceramic plate, gently washed with ethanol and distilled water, respectively, and then dried in the desiccator. The addition of a proper amount of NB is crucial in the synthesis. The use of the exact amount of ZA and NB for each product will be presented in the test.

2. Characterization. Structures of the products were characterized by powder X-ray diffraction (XRD) and electron microscopy. Powder XRD patterns were collected on a diffractometer (Philips PW1830) using $\text{Cu K}\alpha$ radiation ($\lambda = 0.1541 \text{ nm}$) and a graphite monochromator operated at 40 kV and 30 mA. Scanning electron microscopy (SEM) images were taken on a JEOL JSM-6330F field emission scanning electron microscope. Samples were gold-coated

- (9) (a) Yada, M.; Taniguchi, C.; Torikai, T.; Watari, T.; Furuta, S.; Katsuki, H. *Adv. Mater.* **2004**, *16*, 1448–1453. (b) Muhr, H.-J.; Krumeich, F.; Schonholzer, U. P.; Bieri, F.; Niederberger, M.; Gauckler, L. J.; Nesper, R. *Adv. Mater.* **2000**, *12*, 231–234. (c) Krumeich, F.; Muhr, H. J.; Niederberger, M.; Bieri, F.; Schnyder, B.; Nesper, R. *J. Am. Chem. Soc.* **1999**, *121*, 8324–8331. (d) Guo, L.; Liu, C.-M.; Wang, R.-M.; Xu, H.-B.; Wu, Z.-Y.; Yang, S.-H. *J. Am. Chem. Soc.* **2004**, *126*, 4530–4531.
- (10) (a) Ma, R.; Bando, Y.; Sasaki, T. *J. Phys. Chem. B* **2004**, *108*, 2115–2119. (b) Zhang, S.; Chen, Q.; Peng, L. M. *Phys. Rev. B* **2005**, *71*, 14104–14114.
- (11) Li, Y. D.; Li, X. L.; He, R. R.; Zhu, J.; Deng, Z. X. *J. Am. Chem. Soc.* **2002**, *124*, 1411–1416.
- (12) Goldberger, J.; He, R. R.; Zhang, Y. F.; Lee, S. K.; Yan, H. Q.; Choi, H. J.; Yang, P. D. *Nature* **2003**, *422*, 599–602.
- (13) Wang, X. D.; Gao, P. X.; Li, J.; Summers, C. J.; Wang, Z. L. *Adv. Mater.* **2002**, *14*, 1732–1735.
- (14) Kong, X. H.; Li, Y. D. *Chem. Lett.* **2003**, *32*, 1062–1063.
- (15) Cheng, J.-P.; Guo, R.-Y.; Wang, Q.-M. *Appl. Phys. Lett.* **2004**, *85*, 5140–5142.
- (16) Sun, X. W.; Yu, S. F.; Xu, C. X.; Yuen, C.; Chen, B. J.; Li, S. *Jpn. J. Appl. Phys.* **2003**, *42*, L1229–L1231.
- (17) Hu, J. Q.; Bando, Y. *Appl. Phys. Lett.* **2003**, *82*, 1401–1403.
- (18) Jeong, J. S.; Lee, J. Y.; Cho, J. H.; Suh, H. J.; Lee, C. J. *Chem. Mater.* **2005**, *17*, 2752–2756.
- (19) Vayssieres, L.; Keis, K.; Hagfeldt, A.; Lindquist, S. T. *Chem. Mater.* **2001**, *13*, 4395–4398.
- (20) Wang, Z.; Qian, X. F.; Yin, J.; Zhu, Z. K. *Langmuir* **2004**, *20*, 3441–3448.
- (21) Liang, L. F.; Xu, H. F.; Su, Q.; Konishi, H.; Jiang, Y. B.; Wu, M. M.; Wang, Y. F.; Xia, D. Y. *Inorg. Chem.* **2004**, *43*, 1594–1596.
- (22) Wang, X.; Sun, X. M.; Yu, D. P.; Zou, B. S.; Li, Y. D. *Adv. Mater.* **2003**, *15*, 1442–1445.
- (23) Mayers, B.; Xia, Y. N. *Adv. Mater.* **2002**, *14*, 279–282.
- (24) Kong, X. Y.; Wang, Z. L.; Wu, J. S. *Adv. Mater.* **2003**, *15*, 1445–1449.
- (25) (a) Liu, Y.; Dong, J.; Liu, M. *Adv. Mater.* **2004**, *16*, 353–356. (b) Liu, Y.; Liu, M. *Adv. Funct. Mater.* **2005**, *15*, 57–62.
- (26) (a) Wang, X.; Li, Y. D. *Angew. Chem., Int. Ed.* **2003**, *42*, 3497–3500. (b) Rosenfeld Hachohen, Y.; Grunbaum, E.; Tenne, R.; Sloan, J.; Hutchison, J. L. *Nature* **1998**, *395*, 336–337.
- (27) Wang, Z. L. *J. Phys.: Condens. Matter* **2004**, *16*, R829–R858.
- (28) Xing, Y. J.; Xia, Z. H.; Zhang, X. D.; Song, J. H.; Wang, R. M.; Xu, J.; Xue, Z. Q.; Yu, D. P. *Solid State Commun.* **2004**, *129*, 671–675.
- (29) Zhang, X. H.; Xie, S. Y.; Jiang, Z. Y.; Zhang, X.; Tian, Z. Q.; Xie, Z. X.; Huang, R. B.; Zheng, L. S. *J. Phys. Chem. B* **2003**, *107*, 10114–10118.
- (30) Hosono, E.; Fujihara, S.; Kimura, T.; Imai, H. *J. Colloid Interface Sci.* **2004**, *272*, 391–398.
- (31) (a) Hosono, E.; Fujihara, S.; Kimura, T. *Electrochim. Acta* **2004**, *49*, 2287–2293. (b) Hosono, E.; Fujihara, S.; Kimura, T.; Imai, H. *J. Sol-Gel Sci. Technol.* **2004**, *29*, 71–79. (c) Hosono, E.; Fujihara, S.; Kimura, T. *Electrochem. Solid-State Lett.* **2004**, *7*, C49–C51.
- (32) Vanheusden, K.; Warren, W. L.; Seager, C. H.; Tallant, D. R.; Voigt, J. A.; Gnade, B. E. *J. Appl. Phys.* **1996**, *79*, 7983–7990.
- (33) Zhang, J.; Sun, L. D.; Liao, C. S.; Yan, C. H. *Chem. Commun.* **2002**, 262–263.
- (34) Jiang, C. L.; Zhang, W. Q.; Zou, G. F.; Yu, W. C.; Qian, Y. T. *J. Phys. Chem. B* **2005**, *109*, 1361–1363.
- (35) Liu, B.; Yu, S. H.; Zhang, F.; Li, L. J.; Zhang, Q.; Ren, L.; Jiang, K. *J. Phys. Chem. B* **2004**, *108*, 4338–4341.
- (36) Wang, J. M.; Gao, L. J. *Cryst. Growth* **2004**, *262*, 290–294.
- (37) Qiu, Z. R.; Wong, K. S.; Wu, M. M.; Lin, W. J.; Xu, H. F. *Appl. Phys. Lett.* **2004**, *84*, 2739–2741.
- (38) Yu, W. D.; Li, X. M.; Gao, X. D. *Cryst. Growth Des.* **2005**, *5*, 151–155.
- (39) Wang, X. D.; Summers, C. J.; Wang, Z. L. *Nano Lett.* **2004**, *4*, 423–426.
- (40) Baxter, J. B.; Wu, F.; Aydil, E. S. *Appl. Phys. Lett.* **2003**, *83*, 3797–3799.
- (41) Wu, J. J.; Liu, S. C. *Adv. Mater.* **2002**, *14*, 215–218.

- (42) Boyle, D. S.; Govender, K.; O'Brien, P. *Chem. Commun.* **2002**, 80–81.
- (43) Pang, Z. W.; Dai, Z. R.; Wang, Z. L. *Science* **2001**, *291*, 1947–1949.
- (44) Kong, X. Y.; Ding, Y.; Yang, R.; Wang, Z. L. *Science* **2004**, *303*, 1348–1351.
- (45) Li, F.; Ding, Y.; Gao, P. X.; Xin, X. Q.; Wang, Z. L. *Angew. Chem., Int. Ed.* **2004**, *43*, 5238–5242.
- (46) Gao, P. X.; Wang, Z. L. *J. Am. Chem. Soc.* **2003**, *125*, 11299–11305.
- (47) Tian, Z. R.; Voigt, J. A.; Liu, J.; Mckenzie, B.; Mcdermott, M. J.; Rodriguez, M. A.; Konishi, H.; Xu, H. F. *Nat. Mater.* **2003**, *2*, 821–826.
- (48) Tian, Z. R.; Voigt, J. A.; Liu, J.; Mckenzie, B.; Mcdermott, M. J. *J. Am. Chem. Soc.* **2002**, *124*, 12954–12955.
- (49) (a) Poul, L.; Jouini, N.; Fiévet, F. *Chem. Mater.* **2000**, *12*, 3123–3132. (b) Morioka, H.; Tagaya, H.; Kadokawa, J.-I.; Chiba, K. *J. Mater. Sci. Lett.* **1999**, *18*, 995–998.

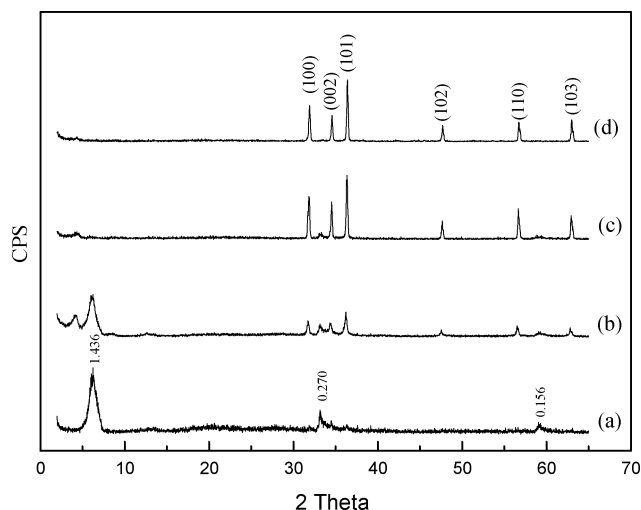


Figure 1. Powder XRD patterns of the products prepared from the mixture with 0.8 mL of NB at 180 °C for (a) 1 h, (b) 2 h, (c) 5 h, and (d) 10 h, respectively.

prior to the SEM analysis. Photoluminescence (PL) was studied on a Fluorolog-3 fluorescence spectrophotometer at room temperature. An ozone-free, 450-W xenon lamp passing through the double-grating excitation and single-grating emission monochromators in a Czerny–Turner configuration was used as the excitation light source.

Results and Discussion

1. Synthesis of Hexagonal ZnO Microboxes. The typical product, formed from the solution with 0.8 mL of V_{NB} at 180 °C after 10 h, was proved by the powder XRD to possess the wurtzite (hexagonal) ZnO structure (Figure 1d). The diffraction of (002) weaker than that of (100) and (101) is typical because of the extinction of (001) diffractions, which is in line with what has been reported in the literature.^{17–19}

The hollow nature inside the nanowalled microboxes was discovered from broken crystals (see Figure 2). Via a close look from the right up-corner, it can be seen that most drumlike microprisms are closed cages with sizes of about tens of microns in both diameter and length. High-magnification SEM images clearly display microcages (see Figure SI-1 in the Supporting Information) that are much different from those of either truncated, hexagon-based polyhedral or spherical ZnO cages with nanoshells formed by textured self-assembly of nanocrystals.⁴⁶

These ZnO microboxes are mainly composed of smooth outer shells, with both tops and bottoms closed by nanoplates. This is quite different from the reported prismatic and hollow

ZnO microtubes that have at least one {001} end opened.^{14–20} Furthermore, the aspect ratios of these microboxes are much smaller than those reported in the literature.^{14–20} Recently, Liu and co-workers reported square-shaped SnO_2 nanoboxes and nanotubes,²⁵ very different from the hexagonal outer geometry observed here. Therefore, the structures of our prismatic closed and drumlike hexagonal ZnO microboxes are quite unique.

Remarkably, the outer faces of the ends look flat, resembling those of ZnO microcolumns described by Baxter et al.⁴⁰ It is interesting that a concave bowl exists at the center of each bottom plate (white arrows, Figure 2), with the protrudent thin walls inclining inward a bit on the edges of each top plate (black arrows, Figure 2). Six edges construct a short prismatic cup erecting on the top. Each hollow ZnO microcrystal is composed of two parts: a hexagonal box with inner caves and a shallow cup with outer caves (Figure 2). The formation of the outer cave in the shape of a cupped cap may be attributed to subsidence due to hollow interiors. Cupped microstructures of ZnO rods were recently made by Qian and co-workers using the precursor of $\text{Zn}(\text{N}_2\text{H}_4)_2\text{Cl}_2$.³⁴ Nonetheless, the structure of our cupped-end microboxes is quite novel.

2. Time Dependence. To understand the growth mechanism, a careful time-dependent growth was conducted. The initial product was confirmed to be the layered hydroxide of ZnAc_2 [LHZA; $\text{Zn}_5(\text{OH})_8(\text{OCOCH}_3)_2 \cdot 2\text{H}_2\text{O}$] (Figures 1a and SI-2 in the Supporting Information).^{30,49}

As shown in Figure 3a, nanoplates assembling beautiful coralline structures were yielded at the initial reaction stage. These nanoplates are about 100 nm thick, with their heights up to 10 μm . The flake morphology of these LHZAs, with a typical hydrozincite structure, has been well described in the literature.^{30,49} The layer slab is composed of zinc hydroxide tetrahedral ZnO_4 and octahedral ZnO_6 , with CH_3COO^- anions intercalated between the positively charged layers of the hydroxide $[\text{Zn}_5(\text{OH})_8(\text{H}_2\text{O})_2]^{2+}$. The LHZA has been used as a precursor to prepare well-defined porous ZnO nanoparticles and porous nanocrystalline ZnO films via a novel base-free route.³¹ Unusual ZnO superstructures with nanosheets standing around a backbone were prepared from flaky hydroxide zinc chloride by a reflux reaction.³⁵ However, synthesis of the “closed-box” type of ZnO structures from these layered compounds was not achieved.

Hexagonal microprisms of ZnO are observed after hydrothermal reaction for 2 h (as shown in Figure 3b), forming

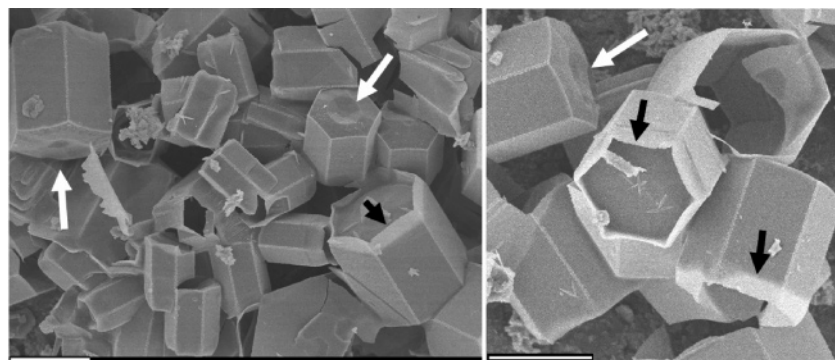


Figure 2. SEM images of hollow and hexagonal ZnO microboxes prepared from the mixture with 0.8 mL of NB at 180 °C for 10 h. The bar is 10.0 μm .

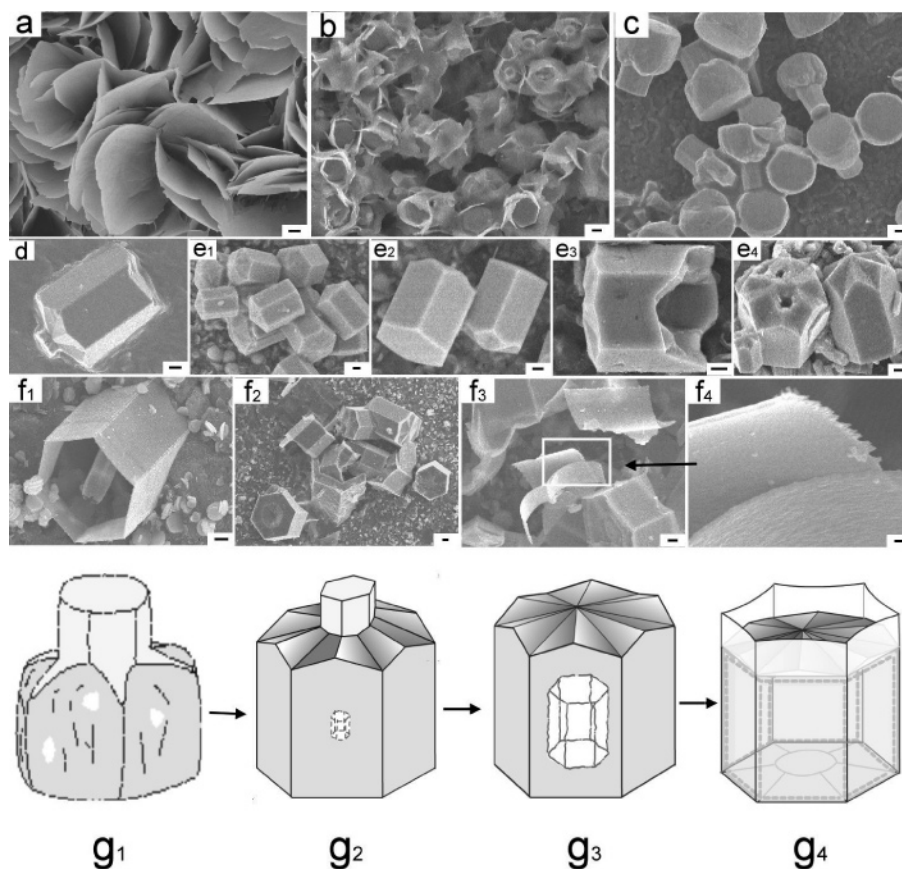


Figure 3. Time-dependent growth progress illustrated by SEM images for samples synthesized for (a) 1 h, (b) 2 h, (c) 3 h, (d) 4 h, (e) 5 h, and (f) 20 h and (g) illustrated schematically. The black bar is 1.0 μm except for that in f_4 , which is 100 nm.

the ZnO microcrystals with the bottom much larger than the top and surrounded by the precursory nanosheets. The powder XRD pattern confirms that the product is a mixture of ZnO and LHZA (Figure 1b).

With a longer time for the hydrothermal treatment, the coating of LHZA gradually disappeared, leading to the formation of translucent ZnO microcrystals (Figure 3c). Clearly, the diameter of the bottom is still larger than that of the top (Figure 3c). Likely, the bottom of the inner prism is convolved by outer shells to form a gourd-shaped ZnO microcrystal (Figure 3c). A few broken ZnO microcrystals illustrate that they are solid with filled interiors.

After a hydrothermal treatment of over 4 h, faceted and hexagonal ZnO microprisms were yielded with fully developed morphologies (Figure 3d). A ZnO crystal holding a smaller hexagonal cap on its top (Figure 3d) can be found. A longer time for the hydrothermal reaction leads to the formation of the “fused” top (parts e_1 and e_2 of Figure 3). This implies that the outer shell on the bottom part grows as the hydrothermal reaction proceeds, lifts up the whole crystals gradually, and then conceals at the top (parts c–e of Figure 3). Further, the outer surface of the top looks quite different from that of the bottom (parts e_1 and e_2 of Figure 3). Each top plane of most crystals is a smooth hexagonal pyramid composed of six triangular plates. The bottom surface, however, is relatively flat. A typical broken ZnO crystal clearly exhibits its hollow nature with a wall thickness

of 200–300 nm (parts e_3 and e_4 of Figure 3). Negligible impurity was observed in this sample (Figure 1c).

After 10 h of reaction, the wall thickness became much thinner (Figure 2) than before. Electron diffraction indicates that these ZnO microboxes are like single crystals. The anisotropic prismatic geometry of the ZnO microboxes, from a structural analysis along $\langle 001 \rangle$ directions, can be assigned to the inherent $P6_3mc$ space group. After an even longer hydrothermal heating, the continuous thinning of the wall eventually transformed the microboxes into separated thin nanosheets with a thickness of about 100 nm (Figure 3f).

The time-dependent growth procedure is summarized schematically in Figure 3g. The above experimental results indicate that LHZA is formed as a kinetic product at the initial step and the hollow structure results from an “elimination” of the inner zinc species⁴⁶ of the microprism in parts d and e of Figure 3. Complete investigations are still underway, and the growth mechanism will be depicted in much more detail in the future.

3. PL. The PL properties of the ZnO microboxes were measured at an excitation wavelength of 267 nm at room temperature. Figure 4 shows a room-temperature PL spectrum of the ZnO microboxes, in which three emissions can be seen. Besides the UV emission that can be attributed to the near-band edge emission of the wide band gap of ZnO, both the blue and green emissions near 442 and 530 nm originated from the crystal defects with different energy levels below the conducting band.^{27–41} This significant

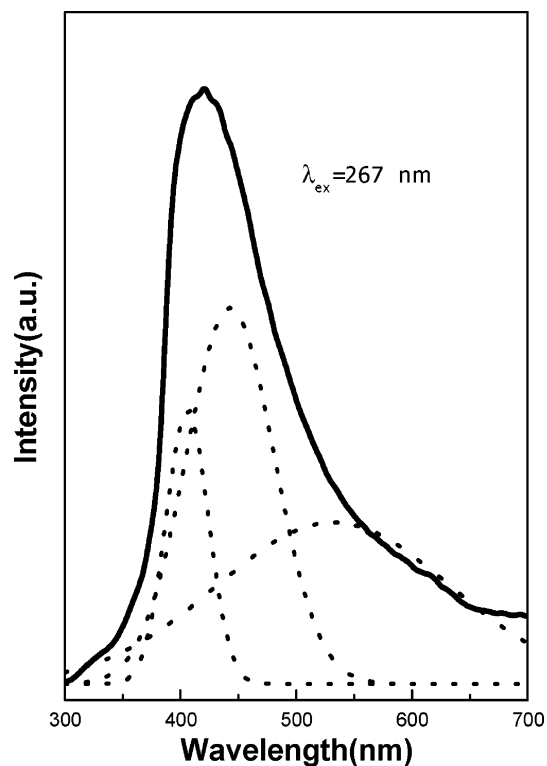


Figure 4. PL of the typical product prepared at 180 °C for 10 h. Three emissions at 400, 442, and 530 nm are isolated.

emission in the visible range might indicate that there could exist abundant crystal defects (oxygen vacancy) in ZnO microboxes with large surface areas potentially good for making new chemical sensors and solar cells.⁵⁰

4. Effect of the NB Concentration. Organic molecules in solution for controlling the morphologies of crystals, a rather old topic in solid-state chemistry, are playing a major role in solution syntheses of inorganic materials of many types. No ZnO was formed before the addition of NB. With an increase in the NB concentration, the yield and outer geometry of the ZnO products were gradually changed. At a lower NB concentration, a very small amount of the ZnO product could be obtained. At a higher NB concentration, for example, when V_{NB} was 1.2 mL, poorly defined ZnO microcrystals including some tubes were formed. At a further higher concentration of NB, no open microboxes were observed, implying that this is the condition in which it is difficult to grow the boxed (tubular) ZnO microcrystals. These experimental results indicate that the amount of NB in hydrothermal synthesis is closely related to the growth patterns and the final morphologies of ZnO microcrystals.

5. Growth of Hollow Hexagonal Microdisks. The reaction temperature is one of the factors that can alter the route for growing ZnO crystals. As the reaction temperature dropped to 140 °C, no hollow structures but mainly nanosheets of LZHA were formed. In the solution with 2.4 mL of NB, hexagonal microcrystals were formed, with their sizes smaller than those formed at 180 °C (Figure 3). It has been well established that the selective adsorption of the

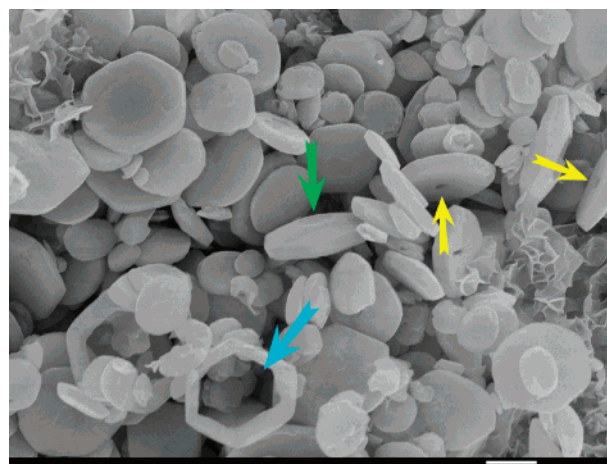


Figure 5. SEM images of the hollow and hexagonal microdisks prepared from a mixture with 2.4 mL of NB at 140 °C for 5 h. The bar is 1.0 μm . organics on ZnO surfaces would prevent certain facets from further growing, resulting in many unusual morphologies for ZnO.^{45,47,48} Obviously, NB significantly inhibited the crystal growth along the $\langle 001 \rangle$ direction. Figure 5 exhibits the hexagonal microdisks, prepared at 140 °C for 5 h, with much smaller aspect ratios. The broken rings indicated by the arrows imply that hollow and closed hexagonal microcages can take a shape mimicking an inorganic fullerene.²⁶ These hexagonal disks and rings of ZnO are quite similar to those most recently reported by Wang and co-workers,⁴⁵ thus inspiring us to refer to both of the microboxes and microdisks (Figures 2 and 5) as ZnO microfullerenes. As compared to the previous pioneering work,⁴⁵ besides these hexagonal disks and rings, microboxes of ZnO have been explored. We might suppose that these rings resulted from the inner “elimination” of zinc species as in the above microboxes.⁴⁶

Conclusion

Top- and bottom-closed, single-crystalline hexagonal microtubes of ZnO exhibiting wide emission in the UV–visible range have been successfully fabricated by a facile, template- and base-free hydrothermal growth. It was found that the reaction temperature and time have great effects on the growths and morphologies of the ZnO crystals. Hollow, hexagonal, and prismatic ZnO microdisks were synthesized at low reaction temperatures and high NB concentrations. The outer geometries of these faceted ZnO microcrystals are closely related to the crystallographic structure of wurtzite with the space group $P6_3mc$. The reaction time and temperature and the use of NB play crucial roles in the growth of the novel microcages and microdisks.

Acknowledgment. This work has been supported by the Natural Science Foundation of China (for distinguished team), NSF of Guangdong for rare-earth luminescence and optoelectronic materials, team program of NSF of Guangdong for optoelectronic materials, and Guangzhou Government for semiconducting materials.

Supporting Information Available: SEM images and physical and chemical analyses. This material is available free of charge via the Internet at <http://pubs.acs.org>.

(50) Law, M.; Greene, L. E.; Johnson, J. C.; Saykally, R.; Yang, P. D. *Nat. Mater.* **2005**, *4*, 455–459.